ULTRAFINE-GRAINED MATERIALS PROCESSED FROM NANOPOWDERS: MICROSTRUCTURES AND MECHANICAL PROPERTIES

G. F. Dirras[1], J. Gubicza[2] and H. Q. Bui[1]

[1]*LPMTM-CNRS, Institut Galilée, Université Paris 13, 99 Avenue J.B. Clément 93430 Villetaneuse, France*
[2]*Department of Materials Physics, Eötvös University, Budapest, P.O.B 32 H-1516, Hungary*

Abstract. Bulk ultrafine-grained materials (Al, Fe, Ni) have been processed either by Hot Isostatic Pressing (HIP), Spark Plasma Sintering (SPS) or combined HIP and dynamic severe plastic deformation (DSPD). The resulting microstructures (grain/crystallite sizes, grain size distribution, crystallographic texture, defects) depend on the processing route and are characterised by means of X-ray diffraction line profile analysis and transmission electron microscopy. The influence of the microstructure on the mechanical behaviour is studied by quasi-static compression test at room temperature. The observed macroscopic behaviour especially the flow softening during the quasi-static compression tests is discussed in relation with the initial microstructure and its evolution during straining.

1. INTRODUCTION

The processing of materials with ultrafine grains strongly expanded in the recent years since the pioneering work of Gleiter [1]. The unique behaviour of these materials opens promising perspectives of their applications in various fields. Nevertheless, it is clear that the strategy for the choice of a material results in a compromise between optimal physical performances for the foreseen application and the capacities of shaping and mechanical strength required. Metals and metallic alloys are the fundamental structural materials. Their properties are strongly dependent not only on the chemical nature of the material, but also on the initial microstructure and on its possible subsequent evolutions under assigned loading or any exterior conditions to face. Consequently, it is of prior importance to control the elaboration process with a deep understanding of the effect of processing conditions on the microstructure and the relationship between the microstructure and the properties of final material.
Among the several ways to process bulk materials with ultrafine grained (ufg) microstructures, the compaction of powders has a fundamental place because of its versatility to tailor microstructures. This type of process allows obtaining fully or near fully dense materials with grain sizes spanning the nanocrystalline (nc, 30-100 nm), the ufg (100 – 1000 nm) and the microcrystalline regimes. nc materials have so far demonstrated excellent physical-chemical properties and improved mechanical characteristics, e.g. high strength [2,3]. Other properties such as ductility which is a key parameter in forming processes are still to be confirmed [4-6]. Indeed, the lack of usable ductility and toughness has slowed down the potential use of these materials in structural components. At the same time, ufg materials processed either by powder metallurgy (PM) methods or severe plastic deformation (SPD) processes or their combination draw an increasing interest as they offer the ways to offset some of the drawbacks exhibited by nc materials [2,3,6-8]. The present work reports on the influence of processing routes on the macroscopic behaviour of bulk ufg materials produced from nanopowders by use of PM methods *per se* or in combination with a SPD process.

2. EXPERIMENTAL PROCEDURES

2.1. Processing routes

Hot Isostatic Pressing (HIP) processing provides a method for producing components from diverse powdered materials, including metals and ceramics. During the HIP process, a powder is placed in a container, typically steel can. The container is subjected to moderate temperature and a very high vacuum to remove air and moisture from the powder. The container is then sealed and HIPed. The application of high inert gas pressures and elevated temperatures results in the removal of internal voids and creates a strong metallurgical bond throughout the material. Fully dense bulk ultrafine-grained aluminium and iron

samples have been processed [9,10] using an instrumented HIP setup. Our HIP device can operate at 1200°C and produces a pressure up to about 300 MPa using Argon as inert gas. The compaction device used in this study has a special expansion cell within the hot press, allowing the measurement of the capsule height or width during compaction, and gives in steadily information on the sample density. It should be noted that HIP is a time-consuming process, particularly with nanopowders as the time needed for removing the gas introduced during the filling step can exceed 1 week for a cylindrical container of 15 mm in diameter and 20 mm height.

Spark Plasma Sintering (SPS) processing has been carried out at the CNRS facilities at Toulouse. The principle of SPS is based on the application of a uniaxial pressure and pulses of high current density to raw powders in a graphite die. The physics of the compaction process is not fully understood, but its main characteristic is an ultra-fast compaction at much lower temperatures than the classical techniques, thus preventing grain growth [11]. In the study reported here, the starting materials were pure Ni nanopowders (80 nm in particle size). The resulting bulk materials have an average grain size of about 300 nm. Nevertheless, microstructure heterogeneity, contamination of the powder or incomplete particles bonding have been reported as shown later on.

Dynamic Severe Plastic Deformation (DSPD) is a peculiar process of severe plastic deformation in the dynamic regime. Dynamic loading offers a remarkable method as a new grain refinement process [12]. Bulk materials produced from coarser powder particles by HIP are subsequently processed using a dynamic drop mass bench with a maximum impact velocity of 10 m/s and of a maximum kinetic energy of 2.5 kJ. The set up apparatus located at L3M (Tremblay Institute of Technology) is equipped with a dynamic load cell, an accelerometer, and a laser beam displacement transducer. In the present study cylindrical pre-Hiped commercial purity (99 %) Al samples have been impacted at a strain rate of $300s^{-1}$. The height reduction was about 70%.

2.2. Mechanical Testing and Microstructure Characterisation

After processing, the resulting materials were subsequently tested by compression at different strain rate in quasi-static regime. The as-processed microstructure and its evolution after compression test were studied by scanning electron microscopy (SEM) coupled with electron backscattering diffraction (EBSD) analysis, transmission electron microscopy (TEM) and X-ray diffraction line profile analysis. The TEM investigation was carried out using a JEOL-2011 operating at 200 kV and the samples were thinned mechanically first to about 50 μm and finally with Ar^+ ions until perforation. The X-ray line profiles are measured by a high-resolution rotating anode diffractometer (Nonius, FR591) using $CuK\alpha_1$ radiation. The scattered X-rays were detected by imaging plates with the angular resolution of 0.005° in 2Θ, where Θ is the angle of diffraction. The line profiles are evaluated using the extended Convolutional Multiple Whole Profile (eCMWP) fitting procedure described in detail in other reports [13,14]. This method gives the dislocation density and the twin-fault probability with good statistics.

3. RESULTS

HIP-processed materials. Figures 1 and 2 illustrate the microstructure and the mechanical behaviour in the case of Al and Fe ufg materials. The Al samples were processed from a powder having mean particle size of 70 nm. Figure 1a shows that HIP resulted in a fully dense bulk material with a composite-like microstructure consisting of micron-sized grains embedded in an ufg matrix with an average grain size of 150 nm and a random crystallographic texture as it is expected from HIP [9]. In Figure 1b the mechanical behaviour during quasi-static compression at a strain rate of about $10^{-4}s^{-1}$ is compared to the behaviour of a conventional Al sample (with the mean grain size of 120 μm) also processed by HIP. A net gain in the yield stress is observed in the case of ufg Al as shown in Figure 1b. It is noticed that after a short plateau, the flow stress slowly decrease ending with a rupture after about 18% plastic deformation. The AFM micrograph presented in Figure 1c shows that the deformation mechanism occurs mainly by multiple events of grain alignments within macroscopic deformation bands homogeneously distributed on the surface of the sample. XRD investigation shown in Figure 1d illustrates the presence of γ-Al_2O_3 particles within the microstructure. The contribution of the oxide phase on the level of yield strength have been evaluated elsewhere [15]. A rough estimation of the amount of the alumina oxide has given about 3% [9].

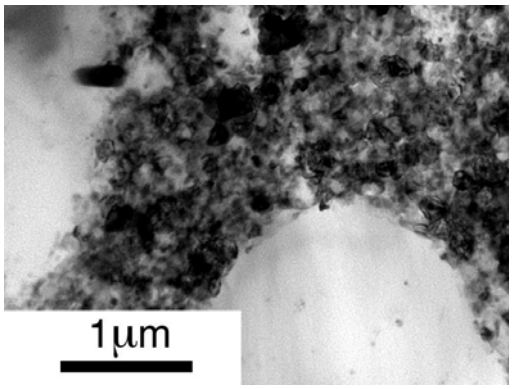

(a)

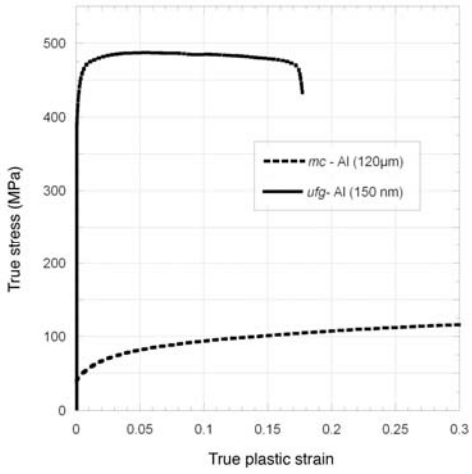

(b)

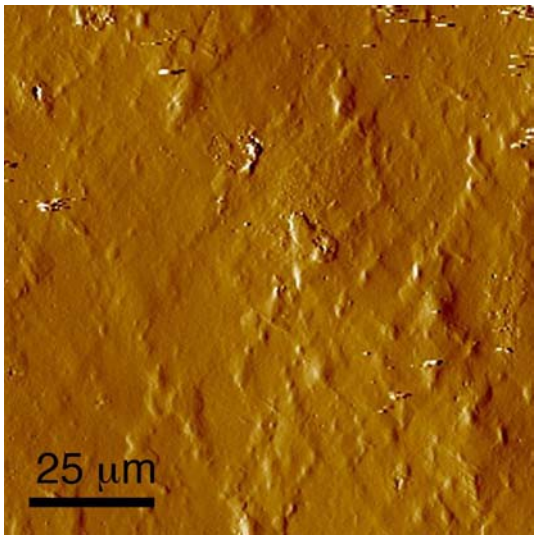

(c)

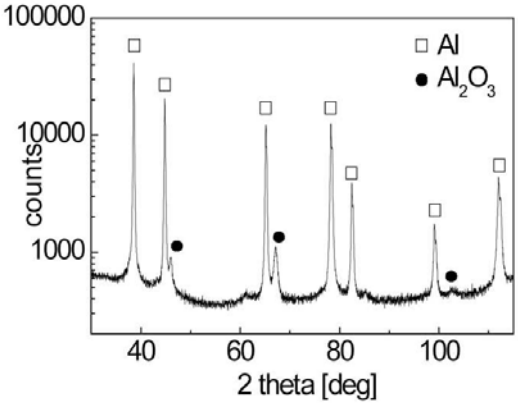

(d)

Figure 1. Different aspects of the microstructure and mechanical behaviour of commercial purity Al processed by HIP. (a): the microstructure of the as-processed bulk material; (b): mechanical behaviour of the ufg material compared to a standard coarse-grained Al; (e): grain alignment during deformation; (d): XRD analysis showing the composite nature of the as-processed material.

Figure 2a shows a comparison of the mechanical behaviour under quasi-static compression of ufg iron samples with different mean grain sizes ranging between 250-1000 nm and a conventional specimen having an average grain size of 5 µm. The jumps in the stress-strain curves are related to strain rate change experiments. The striking feature displayed on the figure is a clear transition occurring at about 500 nm from hardening to softening.

Figure 2b obtained by EBSD experiment shows the microstructure for ufg iron having a mean grain size of 500 nm after the compression test. It is clear that the deformation in the investigated volume mainly occurs in a shear band (SB) located between the two red lines. In this area of Figure 2b, the fraction of small angle grain boundaries is much higher than in its surroundings which indicates a lattice dislocation activity in the SB. The figure also shows the crystallographic texture evolution inside and outside the SB. It can be noticed that while outside the SB the crystallographic texture keeps almost random, a {111} fiber-like texture develops within the SB as a consequence of an intense plasticity.

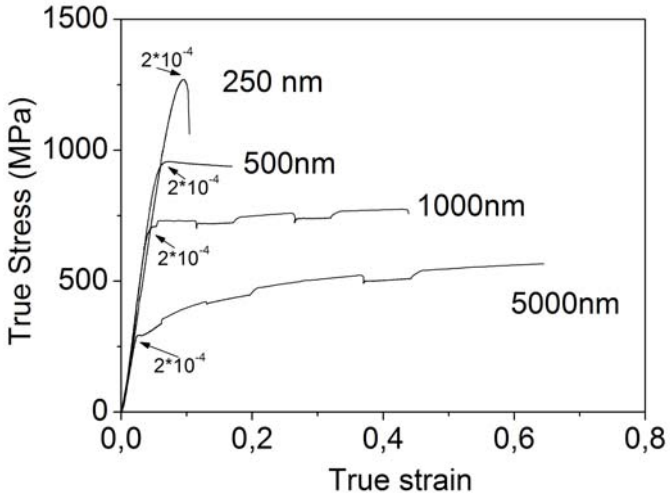

(a)

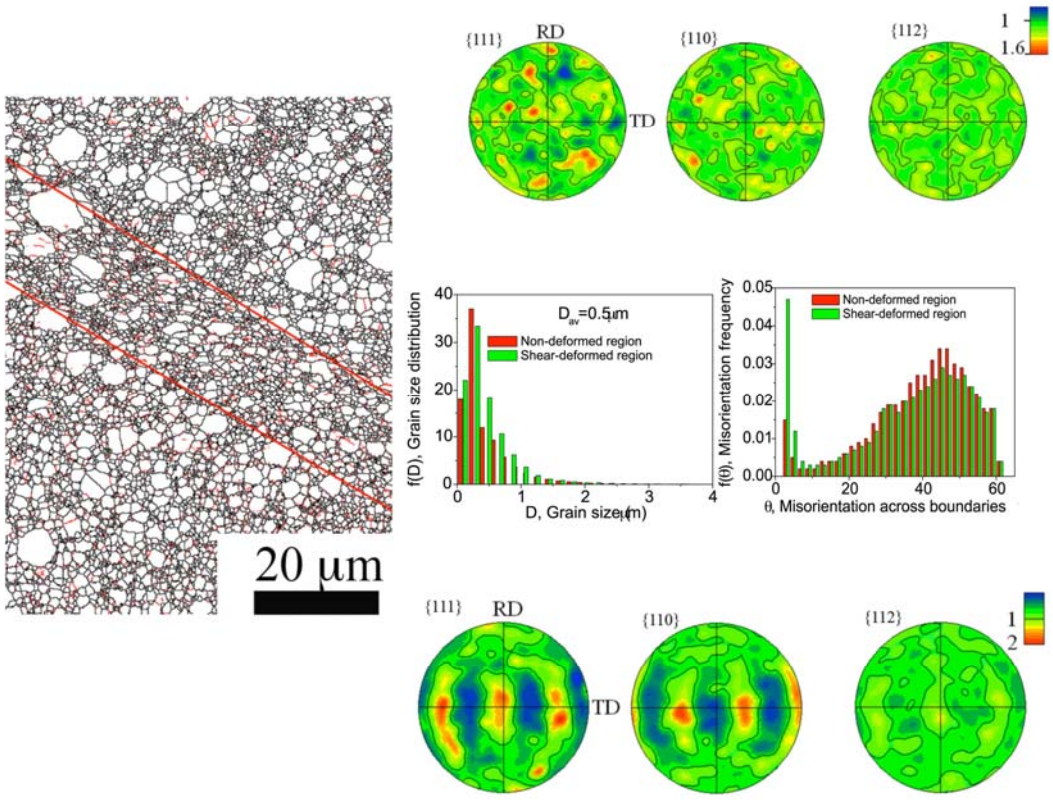

(b)

Figure 2. Mechanical behaviour under quasi-static compression tests of ufg iron processed by HIP (a) and selected microstructure details after compression test for a sample having an average grain size of about 500nm (b). The crystallographic textures inside and outside the SB are shown in the bottom and upper parts of the figure, respectively.

SPS-processed materials. The microstructural features and deformation characteristics of samples processed by SPS (at a pressure and temperature of 150 MPa and 500°C respectively, applied during 1

minutes) are shown in Figure 3. The average grain size is about 294 nm, however the microstructure is heterogeneous in the sense that it contains ufg/nc grains as well as micron-sized grains. TEM images show that a fraction of grains contains grown twins which has an average probability of 0.3% in the whole sample as determined by X-ray line profile analysis. For comparison, another sample was consolidated from the same powder by HIP method. Before HIP processing, the powder was heat-treated in a glove box under controlled hydrogen flux at 400°C and subsequently encapsulated and sealed under inert gas (Ar) for preventing oxidation. During HIP method, the capsule was subjected to a pressure of 140 MPa at 700 °C for 150 min. In the case of SPS, the powder has been processed in air before the sintering which results in a two times higher oxide content compared with the HIP-processed sample as revealed by XRD investigation (not shown here). The average grain size in the case of HIP-processed sample is higher (403 nm) than that for the specimen produced by SPS due to the longer time and higher temperature of HIP processing. The twin probabilities and dislocation densities ($5\text{-}6\text{x}10^{14}$ m^{-2}) are the same in the two materials within the experimental errors. The higher oxide content and the smaller grain size of the SPS-processed sample result in a higher compressive yield strength. X-ray analysis revealed that the dislocation density increased while the twin-probability decreased during compression test indicating dislocation activity during deformation. The decay of twins are also confirmed by TEM. In Figure 3b the arrows indicate locations of incomplete particle bonding in the vicinity of a coarse grain in the SPS-processed sample.
As for the mechanical behaviour, Figure 3c reveals that during compression of the SPS-sample a plateau occurs after a short hardening stage that is immediately followed by a flow softening regime till the failure of the sample. The inset in Figure 3c is a SEM observation showing that the ufg matrix deforms by grain alignment in multiple deformation band events. In addtion, cracks are created at the interfaces between large and ufg grains. Contrary to the SPS-processed Ni sample, flow softening and cracks were not observed for the sample produced from the same initial powder by HIP.

DSPD-processed materials. In this case samples are first prepared by HIP from conventional coarse-grained powders. The resulting grain size in the as-HIPed material was about 2 μm. After the DSPD step the grain size decreases down to about 500 nm as measured by TEM while X-ray line profile analysis gives a dislocation density of about $1.4\pm0.2\text{x}10^{14}$ m^{-2}. This microstructure has been also found to be stable after 3 months storage at room temperature. Figure 4a shows the microstructure of the HIP-processed sample before and after crash-test. After DSPD step the material exhibited a strong {111} fiber-like texture parallel to the impact load axis [12]. Figure 4b illustrates the effect of a strain path change during subsequent quasi-static compression tests conducted parallel to the impact axis (ND) and perpendicular to the impact axis (TD). It is observed that while a long hardening stage is observed when the sample is tested along ND, in the case of TD testing a maximum in the flow stress has been reached at small strains which was followed by a rapid flow softening.

4. DISCUSSION

In this study different ufg materials have been processed using different PM procedures. In spite of the differences in the resulting microstructures, the compression behaviour of all materials can be characterized by a short initial hardening at the very beginning of the deformation which is followed by a lack of hardening or even flow softening. In the following section we are discussing only the apparent softening exhibited by the macroscopic compression behaviour of the processed materials.
Both in the cases of iron and nickel it was found that for large grain size (>500 nm) the samples harden during compression test while for small grains flow softening occurs. Due to the Hall-Petch relation, smaller the grain size, higher the stresses needed for plastic deformation. The higher stress level during deformation results in a larger probability of debonding in the grain boundaries during straining. The resulting cracks may yield to strain localization and flow softening with increasing strain. Moreover, as the smaller grain size of the sintered specimens is usually resulted from smaller initial powder particle size, these samples contain higher oxide content. The higher volume fraction of oxide dispersoids causes an additional increase of the flow stress which may increase the probability of cracking at grain boundaries. Furthermore, the oxide on the interfaces may reduce the grain boundary strength resulting in easier cracking [16]. In the case of Ni processed by SPS, the powder processing in air further increased the oxide content in the sintered sample. Moreover, in this sample there are incomplete particle bonding (see Figure 3b) which may also contribute to cracking during deformation. This explains the different behaviour of Ni samples processed from the same powder by SPS and HIP.

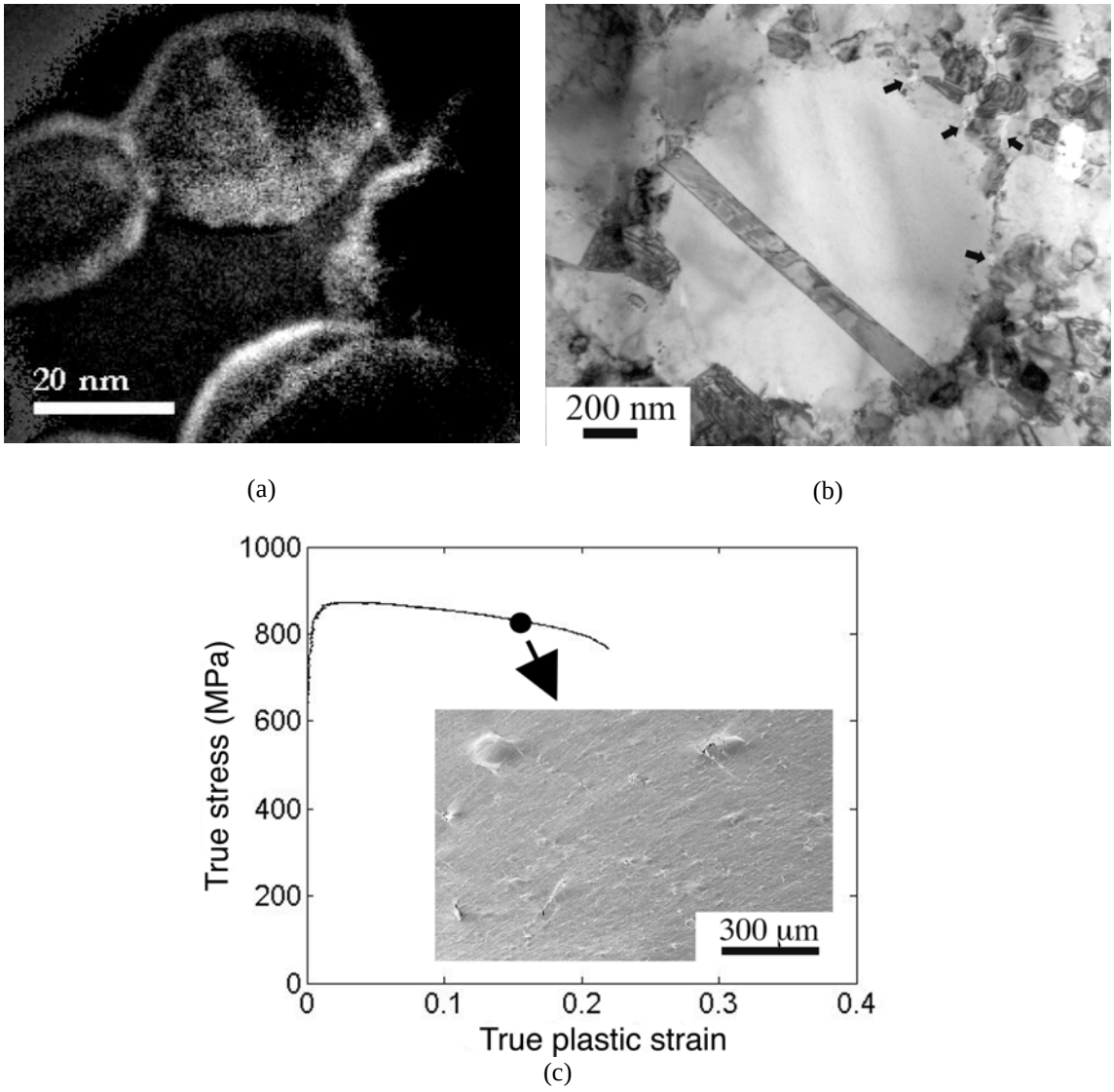

Figure 3. (a): EFTEM image of the starting nanopowder showing a skeleton of NiO on the surface of Ni particles; (b): a typical TEM view of the as processed material. The arrows indicate incomplete particle bonding around a coarser grain; (c): macroscopic behaviour showing a flow softening as a consequence of deformation incompatibility between coarser grains and the ufg matrix.

It is found here that in the face centered cubic (FCC) materials processed by SPS and HIP, the macroscopic deformation of the ufg matrix occurs mostly by grain alignment within thin deformation bands oriented at about 40-45° with the loading axis. These bands are more or less homogeneously distributed. The perfect-like behaviour observed in the case of Al may be explained by the occurrence of these multiple events of grain alignments within deformation bands. It has been reported that the strain rate sensitivity of the flow stress of FCC metals increases with decreasing grain size [17]. It is thus expected that despite the operation of the deformation band a hardening is maintained. Therefore, the rapid decrease of the flow stress observed in the case of SPS processed sample are to be linked to damages nucleated at the interfaces between grains as discussed above.

In the case of DSPD processed samples, a clear strain path change effect is observed. In particular, a marked flow softening is observed during the subsequent quasi-static deformation along TD. This effect has been reported many times in conventional materials [18] and appears to be due to a dynamic destabilization of the microstructure formed during HIP previously. The texture most probably also affects on the

orientation-dependence of compression behaviour. Additional investigations are needed for the full description and understanding of such a behaviour.

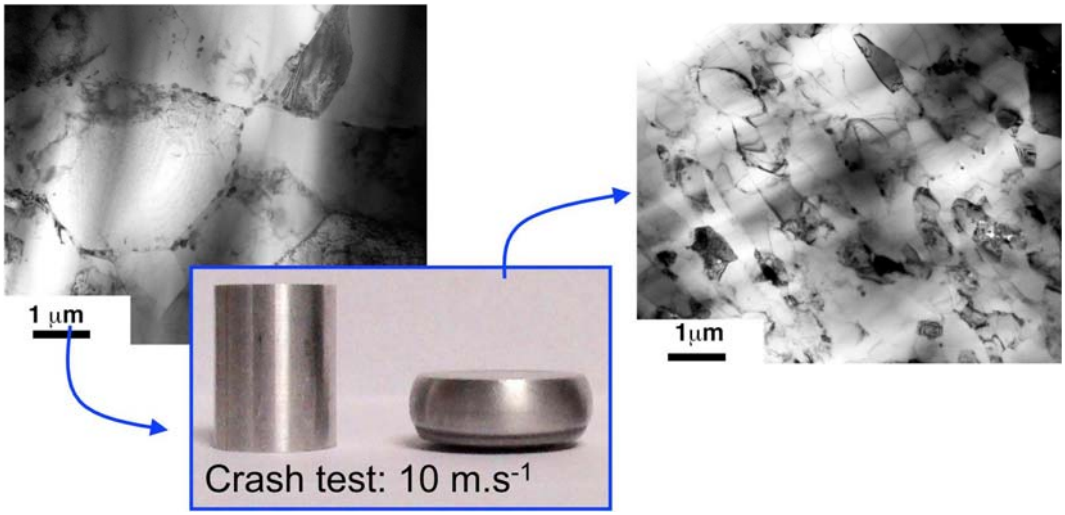

(a)

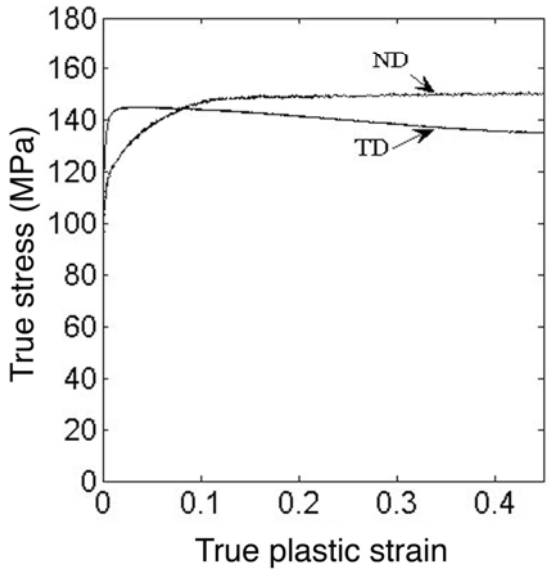

(b)

Figure 4. (a): The microstructure of HIP-processed Al before and after crash-test. (b): mechanical behaviour of the HIP+Crash processed material when the compression axis is parallel (ND) or perpendicular (TD) to the impact direction, simulating the effect of a strain path change.

It should be noted that the transition of the mechanical behaviour from hardening to softening in body centered cubic (BCC) iron has been reported previously [19] following either quasi-static or dynamic compression test. This transition is accompanied by shear band formation that localises the deformation as a consequence of the diminishing strain rate sensitivity of the flow stress with decreasing grain size [17].

5. CONCLUSIONS

In this study the focus has been given on the flow softening observed during quasi-static compression at room temperature conducted on ufg materials processed by different PM routes. It is found that this behaviour is resulted from different origins such as crack nucleation and propagation in the as-sintered samples, or the destabilisation of the sintered microstructures during Dynamic Severe Plastic Deformation or diminishing strain rate sensitivity in the case of iron. Usually the flow softening has been observed for samples having small grain size (<300-500 nm) but the occurrence of this phenomenon is also affected by the oxide content and the incomplete bonding in the as-processed materials.

Acknowledgments
The authors are grateful for the support of the Hungarian TeT Foundation (KPI) under the contract No. F-47/2006 (Balaton project). This work was supported by the Hungarian Scientific Research Fund, OTKA, Grant Nos. K67692 and K71594. JG is grateful for the support of a Bolyai Janos Research Scholarship of the Hungarian Academy of Sciences. GD is grateful for the support of EGIDE, in the framework of the Hubert Curien Project (PHC Balaton). Part of this work was supported by the French network RNMP "AGUF" in collaboration with ARCELOR.

References

[1] Gleiter H., *Prog. Mater. Sci.*, 33 (1989), 223-315.
[2] Kumar, K. S., Van Swygenhoven H., and Suresh S., *Acta Mater*., 51 (2003) 5743-5774.
[3] Youssef, K. M., Scattergood R. O., K., Murty K. L., Koch C. C., *Appl. Phys. Lett*., 85 (2004) 929-931.
[4] Champion, Y., Langlois C., Guérin-Mailly S., Langlois P., Bonnentin J.-L., Hÿtch M. J., *Science*, 300 (2003) 310-311.
[5] Lu, L., Schwaiger R., Shan Z. W., Dao M., Lu K., Suresh S., *Acta Mater*., 53 (2005) 2169-2179.
[6] Youssef, K. M., Scattergood R. O., K., Murty K. L., Horton J. A., Koch C. C., *Appl. Phys. Lett*., 87 (2005) 091904.
[7] Langlois, C., M. Hÿtch, and Y. Lartigue-Korinek,. *Metal. Mater. Trans. A*, 36 (2005) 3451-3460.
[8] Florian H., Dalla Torre, Hänzi A. C., Uggowitzer P. J., *Scripta Mater.*, 59 (2008) 207-210.
[9] Billard S., Fondère J. P., Bacroix B., Dirras G. F., *Acta Mater.*, 54 (2006) 411-421.
[10] Cao W. Q., Benyoucef M., Dirras G. F, Bacroix B., *Mater. Sci. Eng. A* 462 (2006) 100-105.
[11] Paris S, Gaffet E, Bernard F, Munir Z. A., *Scripta Mater.*, 50 (2004) 691-696.
[12] Bui Q. H., Dirras G. F., Hocini A., Ramtani S., Abdul-Latif A., Gubicza J., Chauveau T., *Mater. Sci. Forum* 584-586 (2008) 579-584.
[13] Ribárik G., Gubicza J., Ungár T., *Mater. Sci. Eng*. A 387-389 (2004) 343.
[14] Balogh L., Ribárik G., Ungár T., *J. Appl. Phys*. 100 (2006) 023512.
[15] Gubicza J, Dirras G. F, Szommer P., Bacroix B. *Mater Sci Eng*. A 458 (2007) 385-390.
[16] Kecskes L. J., Cho K. C., Dowding R. J., Schuster B. E., Valiev R. Z., Wei Q. *Mater Sci Eng. A* 467 (2007) 33–43.
[17] Wei Q., Cheng S., Ramesh K. T., Ma E., *Mater. Sci. Eng. A* 381 (2004) 71-79.
[18] Dirras G. F., Duval J.-L., Swiatnicki W. *Mater. Sci. Eng*. A263 (1999), 85–95.
[19] Jia D., Ramesh K. T., Ma E., *Acta Mater*., 51 (2003) 3495-3509.